

Dependence of the superconducting effective mass on doping in cuprates

N.Kristoffel,^{a,b,1} P.Rubin^{a,1}

^a*Institute of Physics, University of Tartu, Riia 142, 51014 Tartu, Estonia*

^b*Institute of Theoretical Physics, University of Tartu, Tähe 4, 51010 Tartu, Estonia*

Abstract

Using a doping-determined multiband model spectrum of a "typical" cuprate the effective mass of the paired carriers is calculated on the whole doping scale. Large m_{ab} values quench rapidly with leaving the very underdoped region. Further slower diminishing of m_{ab} reproduces the trend towards restoring the Fermi-liquid behaviour in cuprates with progressive doping. The interband superconducting condensate density (n_s) shows similar behaviour to the transition temperature and superconducting gaps. The $n_s(0)/m_{ab}$ ratio has an expressed maximum close to optimal doping as also the thermodynamic critical field. All the overlapping band components are intersected by the chemical potential at this. The pairing strength and the phase coherence develop simultaneously. In spite of its simplicity, the model describes the behaviour of various cuprate characteristics on the doping scale.

PACS: 74.20.-z; 74.72.-h

Key words: Cuprate; Two-band model; Effective mass; Doping; Penetration depth

1 Introduction

The superconducting condensate density (n_s) characterizes the order parameter of this macroscopic quantum commonwealth. The way to cuprate high- T_c superconductivity includes (necessarily) a doping treatment. The nature of the reorganizations in the physical-chemical basis of the material and the variation of the superconducting properties on the

¹ Corresponding authors: Tel: +372 742 8164; fax: +372 738 3033; E-mail: kolja@fi.tartu.ee (N.Kristoffel), rubin@fi.tartu.ee (P.Rubin)

doping scale become of primarily interest. At present there remain nevertheless some debatable aspects in the cuprate superconductivity until the pairing mechanism itself. Correspondingly this concerns also the behaviour of the superconducting condensate density on doping, e.g. [1,2].

An essential property which determines numerous applications of superconductors is the penetration depth. It contains n_s with the superconducting condensate effective mass m in the combination m/n_s . The doping dependence of the superconductivity playground CuO_2 plane m_{ab} in cuprates is practically unknown. Usually one supposes a constant value $m \sim xm_0$, with x between, say, 2 and 5 (m_0 is the free electron mass). The main aim of the present contribution is the calculation of m_{ab} on the whole scale of the hole doping (p) in association with other cuprate superconductivity characteristics.

We use a very simple, partly postulative model of a "typical" cuprate superconductor which uses only general knowledge on the system. The model has been started by Ref. [3,4] and developed in [5-7]. The following comparison of the outcome of the model for various properties with the observations is expected to illuminate in some extent the background physics.

The model supports on the two-component scenario of cuprate superconductivity [8,9] which states the essential functioning of the doping-created defect subsystem besides the itinerant one. This means that the background electron spectrum shows essential dynamics under doping. Bare normal state gaps are assumed between the mentioned subsystems and supposed to be quenched by progressive doping. Overlap dynamics of the bands appears now as a novel source of critical doping concentrations. The nature of the minimal quasiparticle excitation energies changes with doping in accordance with the chemical potential position. This explains naturally the presence of pseudogaps in the model. The pseudogaps appear as precursors on the doping scale (not on the energetic one) to the superconducting gaps and survive for $T > T_c$ as normal state gaps.

The pairing interaction is supposed to be of interband pair transfer [10] type between the itinerant and defect states. This mechanism is seemingly the most effective in serving high transition temperatures in a simple way [11,12].

The calculated phase diagram of cuprate energetic characteristics (T_c , superconducting- and pseudogaps, the condensation energy) [5,6] agree qualitatively well with the experimental results. Controversial statements in the literature on interrelations and coexistence of various gaps in distinct doping regions have been elucidated. Compounds with two or one pseudogap in the charge channel can be described.

2 The physical model

We proceed with the description of the physical content of the model background used. It enables the understanding of the behaviour of the characteristics investigated. The cuprate

electron spectrum created and reorganized by doping is chosen as follows. The mainly oxygen itinerant valence band (γ) top fixes the energy zero and this band extends until $\xi = -D$. The states in it are normalized to $1 - c$, where c is a measure of the doped hole concentration (p). The corresponding scaling for a given case must be made by joining a characteristic concentration on the phase diagram. There is a huge (e.g. [13-17]) amount of appointments that doping creates new defect (midband) states near the top of the valence band in the charge-transfer gap. Extended doping brings them to merge with the valence band. The functioning of the defect subsystem is anisotropic in the momentum space [18]. At least the "hot" $(\pi, 0)$ -type and "cold" $(\frac{\pi}{2}, \frac{\pi}{2})$ -type regions must be distinguished. Accordingly we introduce two defect system subbands characterized by energy intervals $d_1 - \alpha c$ and $d_2 - \beta c$, i.e. they expand down from energies at $c = 0$. The overlap of these bands with the valence band is reached at $c_\alpha = d_1\alpha^{-1}$ and $c_\beta = d_2\beta^{-1}$. Note that the infrared manifestations of the defect subsystem are suppressed in favour of the free carriers (Drude peak appearance) with progressive doping [19]. We take d_1 and d_2 to be positive: the optical charge-transfer gap is reduced by doping [20]. The choice $c_\beta < c_\alpha$ accounts for that the lowest doping-created states belong to the cold subsystem. The weight of the defect states is taken to be $c/2$, cf. [17].

The 2D (CuO_2 planes) densities of states in the bands read $\rho_\alpha = (2\alpha)^{-1}$, $\rho_\beta = (2\beta)^{-1}$, $\rho_\gamma = (1 - c)D^{-1}$. There are the following different arrangements of the bands and the chemical potential (μ). At very underdoping $c < c_\beta$, $\mu_1 = d_2 - \beta c$ is connected with the "cold" β -band and charge carriers become concentrated here, cf. [13]. For $c > c_\beta$, $\mu_2 = (d_2 - \beta c)[1 + 2\beta(1 - c)D^{-1}]^{-1}$ intersects both (β, γ) -bands. The Fermi level shifts into the valence band, cf. [21]. The overlap of the narrow defect β -band with the itinerant band leads to the formation of two sheets of the Fermi surface. The one at $(\frac{\pi}{2}, \frac{\pi}{2})$ is holelike with the dominating itinerant contribution and the other with a tendency to form an electronlike "flat band" with lowering μ . This behaviour is in agreement with the observation of two Fermi-sheets [22] and of a single "hole barrel" at $(\frac{\pi}{2}, \frac{\pi}{2})$ [23] and a flatband at $(\pi, 0)$ [24].

For the expressed dopings larger than c_0 , determined by $d_1 - \alpha c_0 = \mu_2$, the role of the $(\pi, 0)$ -type region increases essentially as also Refs. [25,26] state. Now $\mu_3 = [\alpha d_2 + \beta d_1 - 2\alpha\beta c][\alpha + \beta + (1 - c)2\alpha\beta D^{-1}]^{-1}$ intersects all three overlapping bands. For extended overdoping $c > c_1$, where c_1 is defined by $d_2 - \beta c = \mu_3$, the chemical potential $\mu_4 = (d_1 - \alpha c)[1 + 2\alpha(1 - c)D^{-1}]^{-1}$ falls out of the cold defect band. The chemical potential is not affected significantly by pairing and its general trend agrees with the results of special investigations [27-29].

3 Necessary formulas

Our basic Hamiltonian with the coupling (W) of itinerant and defect subsystems by the pair-transfer interaction reads

$$H = \sum_{\sigma, \vec{k}, s} \epsilon_\sigma(\vec{k}) a_{\sigma, \vec{k}, s}^+ a_{\sigma, \vec{k}, s} + W \sum_{\sigma, \sigma'}' \sum_{\vec{k}, \vec{k}'} \sum_{\vec{q}} a_{\sigma \vec{k} \uparrow}^+ a_{\sigma(-\vec{k}+\vec{q}) \downarrow}^+ a_{\sigma'(-\vec{k}'+\vec{q}) \downarrow} a_{\sigma' \vec{k}' \uparrow}. \quad (1)$$

Here $\epsilon_\alpha = \xi_\sigma - \mu$, s is the spin index, σ counts the bands and \vec{q} is the pair momentum with the components from the same bands. Various aspects of the work with (1) at $\vec{q} = 0$ for calculating the superconductivity energetic characteristics can be followed in [3,5,10]. The superconductivity gap parameters are defined as

$$\begin{aligned}\Delta_\gamma &= 2W \sum_{\vec{k}, \tau}^\tau \langle a_{\tau\vec{k}\uparrow} a_{\tau-\vec{k}\downarrow} \rangle, \\ \Delta_\tau &= 2W \sum_{\vec{k}} \langle a_{\sigma-\vec{k}\downarrow} a_{\sigma\vec{k}\uparrow} \rangle,\end{aligned}\tag{2}$$

where \sum^τ means the integration with the densities $\rho_{\alpha,\beta}$ over the corresponding energy intervals of the defect system subbands ($\tau = \alpha, \beta$; $\Delta_\alpha = \Delta_\beta$). The nongapped nature of the cold subsystem [18] can be accounted by the multiplication of Δ_α with the suitable d -symmetry factor.

The gap equation reads ($\theta = k_B T$)

$$\begin{aligned}\Delta_\sigma &= W \sum_{\vec{k}, \tau}^\tau \Delta_\tau(\vec{k}) E_\tau^{-1}(\vec{k}) th \frac{E_\tau(\vec{k})}{2\theta} \\ \Delta_\tau &= W \sum_{\vec{k}} \Delta_\gamma(\vec{k}) E_\gamma^{-1}(\vec{k}) th \frac{E_\gamma(\vec{k})}{2\theta}\end{aligned}\tag{3}$$

with the usual form of the quasiparticle energies $E_\sigma(\vec{k}) = \sqrt{\epsilon_\sigma^2(\vec{k}) + \Delta_\sigma^2(\vec{k})}$. The density of the paired carriers is

$$n_s = \frac{1}{2} \left[\sum_{\vec{k}} \frac{\Delta_\sigma^2(\vec{k})}{E_\sigma^2(\vec{k})} th^2 \frac{E_\sigma(\vec{k})}{2\theta} + \sum_{\vec{k}}^\tau \frac{\Delta_\tau^2(\vec{k})}{E_\tau^2(\vec{k})} th^2 \frac{E_\tau(\vec{k})}{2\theta} \right].\tag{4}$$

The free energy corresponding to the Hamiltonian (1) has been calculated in [30] (see also [7]), where the paired carrier effective mass isotope defect has been investigated. The "soft" order parameter [30] with the critical behaviour at T_c is characterized by the effective mass

$$m_{ab} = \frac{1}{2} \frac{(\eta_\alpha + \eta_\beta + \eta_\gamma)(\delta_\alpha + \delta_\beta + \delta_\gamma)}{(\eta_\alpha + \eta_\beta)\delta_\gamma m_\gamma^{-1} + \eta_\gamma(\delta_\alpha m_\alpha^{-1} + \delta_\beta m_\beta^{-1})},\tag{5}$$

where $m_\sigma = 2\pi\hbar^2\rho_\sigma V^{-1}$, and $V = a^2$ for the CuO_2 plaquette. For $\mu - s$ being not too close to limiting energies $\Gamma_{0\sigma}$ and $\Gamma_{c\sigma}$ of the bands the following formulas for the quantities entering (5) can be used

$$\eta_\sigma = W\rho_\sigma \ln \left[\left(\frac{2\gamma}{\pi} \right)^2 \theta_c^{-2} |\Gamma_{0\sigma} - \mu| |\Gamma_{c\sigma} - \mu| \right],\tag{6}$$

$$\delta_\sigma = \frac{7}{2}\zeta(3)W\rho_\sigma|\mu - \Gamma_{0\sigma}|(\pi\theta_c)^{-2}, \quad (7)$$

when μ is located in the integration region ($\zeta(x)$ is the zeta-function; $\gamma = \exp(0.577)$).

If μ lies out of the band $\delta_\sigma = 0$ and

$$\eta_\sigma = W\rho_\sigma \ln \left| \frac{\Gamma_{c\sigma} - \mu}{\Gamma_{0\sigma} - \mu} \right|. \quad (8)$$

According to (5) the supercarrier effective mass depends on the position of the spectral components and the chemical potential at a given doping. The mixed nature of the excitations in the multiband model is reflected in the expression (5). With the approximations used m_{ab} is temperature independent.

4 Calculated doping dependences

The calculations of T_c , superconductivity gaps, etc. have been made by numerical integration using a plausible parameter set of Ref. [5]. The doping dependences of the cuprate energetic characteristics are illustrated in [5,6]. Here we represent the zero-temperature superfluid density and the condensation energy in Fig.1 *vs.* hole doping $p = 0.28c$ (it has been taken $p = 0.16$ for the $T_c(max)$). The condensation energy is represented by the thermodynamic critical field as

$$H_{c0} = \sqrt{4\pi[(\rho_\alpha + \rho_\beta)\Delta_\alpha^2 + \rho_\gamma\Delta_\gamma^2]}. \quad (9)$$

The bell-like curves of T_c , Δ_σ [5,6], n_s and H_{c0} show the similar behaviour in agreement with the results of [2,31]. Our calculation of the ξ_{ab} correlation length *vs* p has given a valley-profile like curve [7]. The second critical field $H_{c2}(0)$ calculated from ξ_{ab} has also a well expressed maximum [7]. In this manner the strength of the pairing and the phase coherence develop and vanish simultaneously in our model. Analogous conclusion has been done in a number of recent investigations [1,2,32-35]. The T_c maximum peak on the doping scale is a result of the electron spectrum doping-driven dynamics which brings all the band components into overlap at the Fermi energy. Bands overlap dynamics appears as a novel source of critical doping concentrations. In the normal state at c_β and c_0 insulator-to-metal (in the cold and hot subsystems, respectively) are expected to appear. This is in agreement with the observations [2,36,37]. At c_0 also the large pseudogap vanishes, cf. [1,2], due to this overlap. The following overdoped regime corresponds to higher carrier concentrations but to smaller superconducting carrier concentrations. The scatterings which cause pairing by the interband mechanism are reduced here.

It must be also mentioned that the bare itinerant – defect gaps are not manifested in the superconducting density curve because the interband nature of the pairing.

The $n_s(T)$ dependence is illustrated in Fig.2 and describes also the penetration depth

$$\lambda = \left[\frac{xm_0c^2a^2l}{4\pi e^2n_s(T)} \right]^{1/2} \quad (10)$$

dependence on temperature. Here m_{ab} is expressed through the free electron mass m_0 as $m_{ab} = xm_0$ and l is the c-axis lattice constant.

The doping-dependence curve of the paired carrier effective mass is given in Fig.3. To the authors knowledge it has not been obtained earlier. It is seen that m_{ab} cannot be assumed to be constant on the whole doping scale. However, in the actual region of remarkable T_c values, a rough estimation near $x \sim 3$, as often supposed, can be considered as acceptable for estimations. It must be stated that the parameter set used can serve only plausible estimations on the quantitative level.

The large values of x at very underdoping correspond to the large effective mass of the narrowest defect β -band. Starting from c_β the contribution of the wide valence band carriers is continuously added. The kink at c_0 corresponds to the simultaneous action of the $\alpha - \beta$ carriers. The essential decrease in m_{ab} after reaching c_1 is connected with the vanished contribution of the heaviest β -carriers. The superconducting carrier effective mass reflects the structure of the electron spectrum and reproduces the well known trend of the superconducting collective towards the normal Fermi liquid behaviour with doping in cuprates.

The essential ratio $n_s(0)/x$ determining the inverse penetration depth squared is shown *vs* doping in Fig.4. The superfluid density bell-like dependence dominates over the effective mass changes. As the result, λ^{-2} is characterized by a curve with a well expressed maximum on the doping scale. This is in agreement with the experimental findings [1,2,32]. The peaked behaviour of $n_s(0)/m_{ab}$ is a natural consequence of the interband superconductivity. This answers the question rised in Ref. [1] about the decrease of n_s at overdoping. The sublinear T_c *vs* n_s (or λ^{-2}) plot at underdoping, which has been observed in a number of investigations [1,38], is reproduced also by the present model – Fig.5.

Having in mind the results obtained for the energetic characteristics of cuprates [3-6] and the coherence length [7], the results of the present work, and also for the effect of photodoping [39], one can conclude that the model under consideration, despite of its simplicity, is able to describe the cuprate charge-channel associated properties on the whole doping scale.

The spin-channel effects are out of the scope of the model at present. However, there seems to be some correspondence with the models like [40] where the magnetic properties become explained. The ability of the authors model to reproduce qualitatively the behaviour of various cuprate superconducting characteristics on doping is expected to stimulate to fill it in with precised suppositions and quantitative refinements.

Acknowledgement

This work was supported by Estonian Science Foundation grant No 6540.

References

- [1] C. Bernhard et al., Phys. Rev. Lett. **86** (2001) 1614.
- [2] J.L. Tallon et al., Phys. Rev. B **68** (2003) 180501(R).
- [3] N. Kristoffel, P. Rubin, Physica C **356** (2001) 171; Solid State Commun. **122** (2002) 265.
- [4] N. Kristoffel, P. Rubin, Eur. Phys. J. B **30** (2002) 495.
- [5] N. Kristoffel, P. Rubin, Physica C **402** (2004) 257.
- [6] N. Kristoffel, P. Rubin, Proc. Estonian Acad. Sci. Phys. Math. **54** (2005) 98; cond.-mat./0408574v1 (2004).
- [7] N. Kristoffel, T. Örd, P. Rubin, cond.-mat./0504431v1 (2005).
- [8] K.A. Müller, Physica C **341-348** (2000) 11.
- [9] D. Mihailovic, K.A. Müller, in Proceedings of the NATO ASI Materials Aspects of High- T_c Superconductivity, Kluwer, Dordrecht, 1997, p.1.
- [10] N. Kristoffel, P. Konsin, T. Örd, Riv. Nuovo Cim. **17** (1994) 1.
- [11] H. Suhl, B.T. Matthias, L.R. Walker, Phys. Rev. Lett. **3** (1959) 552.
- [12] V.A. Moskalenko, Fiz. Met. Metalloved. **8** (1959) 503.
- [13] A. Ino et al., Phys. Rev. B **65** (2002) 094504.
- [14] Y. Ando et al., Phys. Rev. Lett. **87** (2001) 017001.
- [15] H. Ihara, Physica C **364-365** (2001) 289.
- [16] C.C. Homes et al. Phys. Rev. B **67** (2003) 184516.
- [17] A.A. Borisov , V. A. Gavrichkov, S. G. Ovchinnikov, Modern Phys. Lett. B **17** (2003) 479.
- [18] T. Timusk, B. Statt, Rep. Progr. Phys. **62** (1999) 61.
- [19] P. Calvani, phys. stat. sol. b **237** (2003) 194.
- [20] Y. G. Zhao et al., Phys. Rev. B **63** (2001) 132507.
- [21] H. Romberg et al., Phys. Rev. B **42** (1990) 8768.
- [22] P.V. Bogdanov et al., Phys. Rev. B **64** (2001) 180505.
- [23] J. Mesot et al., Phys. Rev. B **63** (2001) 224516.
- [24] Y. Yoshida et al., Phys. Rev. B **63** (2001) 220501.
- [25] A.D. Gromko et al., Phys. Rev. B **68** (2003) 174520.
- [26] S. Sugai et al., Phys. Rev. B **68** (2003) 184504.
- [27] A. Ino et al., Phys. Rev. Lett. **79** (1997) 2101.
- [28] T. Tohyama, S. Maekawa, Phys. Rev. B **67** (2003) 092509.
- [29] N. Harima et al., Phys. Rev. B **67** (2003) 172501.
- [30] T. Örd, N. Kristoffel, phys. stat. sol. b **216** (1999) 1049.
- [31] T. Schibauchi et al., Phys. Rev. Lett. **86** (2001) 5763.
- [32] D.L. Feng et al., Science **289** (2000) 277.
- [33] T. Schneider, Physica B **326** (2003) 289.

- [34] M.R. Trunin, Yu. A. Nefyodov, A.F. Shevchun, Phys. Rev. Lett. **92** (2004) 067006.
- [35] R. H. He et al., Phys. Rev. B **69** (2004) 220502(R)
- [36] F. Venturini et al., Phys. Rev. Lett. **89** (2002) 107003.
- [37] X.F. Sun, K. Segawa, Y. Ando, Phys. Rev. Lett. **93** (2004) 107001.
- [38] Y.J. Uemura et al., Phys. Rev. Lett. **66** (1991) 2665.
- [39] N. Kristoffel, P. Rubin, Physica C **418** (2005) 49.
- [40] A.S. Alexandrov, P.P. Edwards, Physica C **331** (2000) 97.

Figure captions

Fig. 1. The superfluid density (full line) and the thermodynamic critical field (dashed line) on the doping scale.

Fig. 2. The dependence of the superconducting density on temperature for the doping $p = 0.14$.

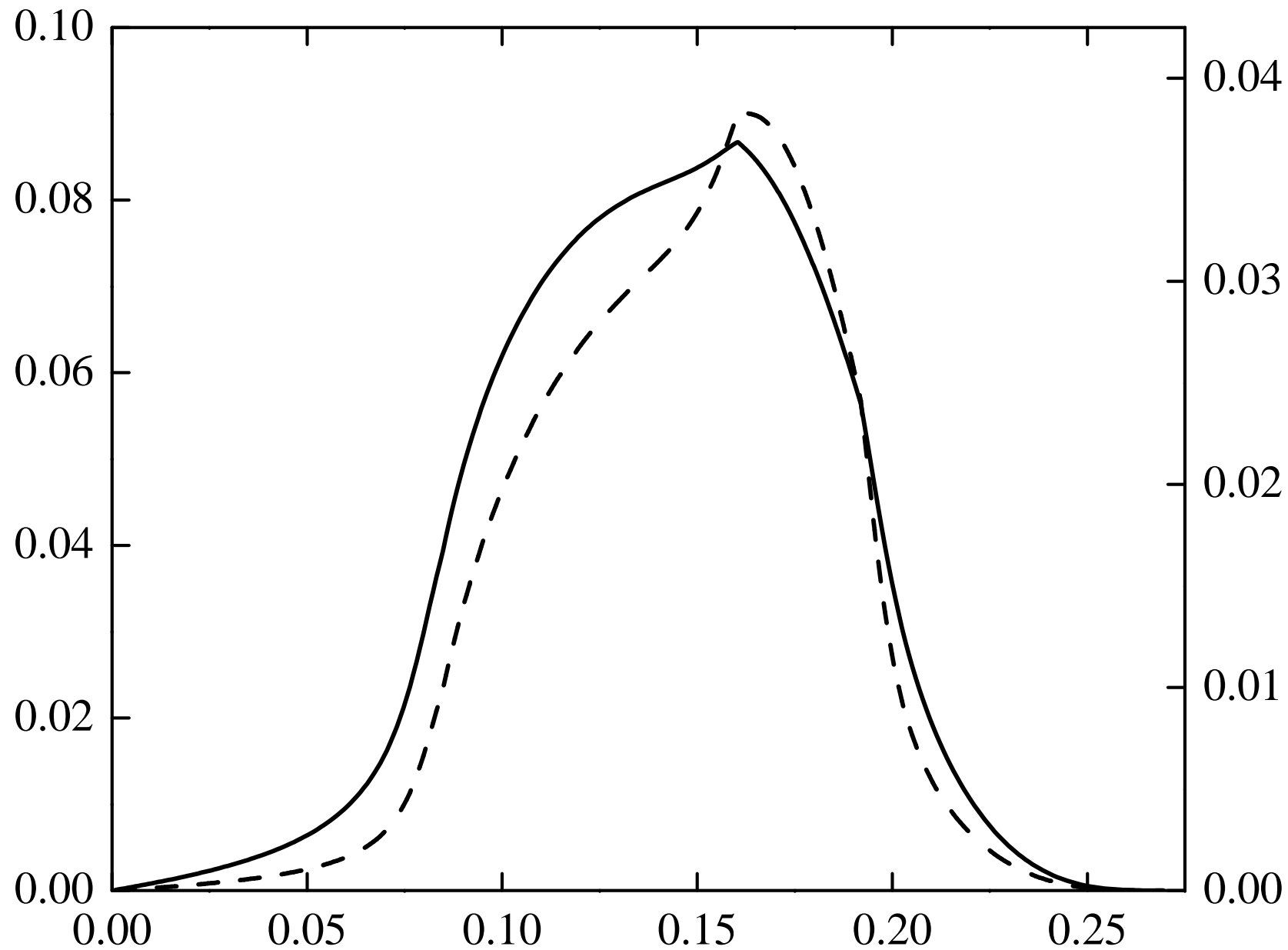
Fig. 3. The supercarrier effective mass dependence on doping.

Fig. 4. The inverse penetration depth squared *vs* doping represented by $n_s(0)/x$; $m_{ab} = xm_0$.

Fig. 5. The Uemura type plot.

$H_c(0)$ ($\text{eV}^{-1/2}$)

n_s



p

